In vitro Evaluation of Lytic Phages for Carbapenem-Resistant *Klebsiella pneumoniae* Isolates

Na Li[1#], Yigang Zeng[2#], Yiyuan Zhang[2], Rong Bao[1], Bijie Hu[1], Tongyu Zhu[1], Demeng Tan[2*]

[1]Zhongshan Hospital, Fudan University, Shanghai, China

[2]Shanghai Public Health Clinical Center, Fudan University, Shanghai, China

[#]These authors contributed equally: Na Li, Yigang Zeng

***Correspondence: Demeng Tan (demengtan@gmail.com)**

Abstract

Klebsiella pneumoniae is a dominate cause of sever community-acquired and nosocomial infections, specifically among immunocompromised individuals. The increasing occurrence of multidrug-resistant (MDR) isolates has significantly impacted the effectiveness of antimicrobial agents. As we have entered the post antibiotic era, the use of bacteriophages to treat pathogenic bacterial infections is becoming revitalized. Elucidating molecular details of phage-bacteria interactions will provide insights into phage biology and better development of phage therapies. In this study, a total of 22 non-duplicate *K. pneumoniae* isolates were assessed for their genetic and phenotypic relatedness by multi-locus sequence typing (MLST), endonuclease *S1* nuclease pulsed-field gel electrophoresis (S1-PFGE) and *in vitro* antibiotic susceptibility testing. Further, the beta-lactamase gene (bla_{KPC}) was characterized to determine the spread and outbreak of *K. pneumoniae* carbapenemase (KPC)-producing enterobacterial pathogens. Three phages were isolated and characterized to evaluate the application of lytic phages against these 22 ST11 *K. pneumoniae* isolates. *In vitro* inhibition assays demonstrated the lytic potential of three relatively broad host-range phages, imposing strong selections for phage-resistant mutants. Comparative genomic sequence analyses revealed that phage-resistant mutants harbored mutations in gene *wcaJ,* which is essential for the biosynthesis of colanic acid. Together, this data suggests that *in vitro* characterization of phage-host interactions adds more comprehensive knowledge to known anti-phage defense strategies and further emphasizes their complexity and future challenges to overcome prior to using phages for controlling this important MDR bacterium.

Keywords: Bacteriophage; Phage therapy; *Klebsiella pneumoniae*; Phage-host interactions; Phage-resistance mechanisms

44 **1. Introduction**

45 The ongoing explosion of the antimicrobial resistance crisis has been accelerated by the overuse
46 and misuse of antibiotics, causing the emergence and increased prevalence of multidrug-
47 resistant (MDR) bacteria [1]. *Klebsiella pneumoniae*, a Gram-negative *Enterobacterales*, can be
48 found in the environment and has been associated with community-acquired infections [2]. The
49 increasingly common mechanism of carbapenem resistance in *K. pneumoniae* is mediated by
50 extended-spectrum β-lactamases (ESBLs), which are able to break the β-lactam structure in the
51 most commonly used antibiotics [3]. Thus, infections of *K. pneumoniae* carbapenemase (KPC)-
52 producing bacteria are consistently associated with poor clinical outcomes and represent a
53 significant and continued threat to the healthcare system. As this problem continues to grow,
54 there is a strong need to find an alternative means to conventional antimicrobials in order to
55 combat this clinical pathogen.

56 Bacteriophages (phages for short) are the most common and diverse biological entities in the
57 biosphere, playing an important role in promoting the bacterial diversity, structuring community
58 composition and being a key driver in nutrient turnover [4]. Lytic phages infect and lyse bacterial
59 hosts and are an attractive alternative towards combating the fast development of antibiotic-
60 resistant *K. pneumoniae* [5, 6]. The use of phages has gained interest over the past years and
61 phages that are specific for MDR bacterial pathogens, including *P. aeruginosa*, *Enterococcus*
62 spp., *Mycobacterium abscessus*, *S. aureus*, *K. pneumoniae*, *A. baumannii*, and *E. coli* have been
63 identified and used to treat bacterial infections [7-14]. These studies demonstrated that lytic
64 phages can be harnessed to prevent and eradicate pathogenic bacteria, and in some cases,
65 alleviate current medical challenges posed by antibacterial resistance and thus further reduce
66 mortalities.

67 While previous applications of phage therapy have shown promising results, the technology is
68 still in a stage of development due to rapid evolution dynamics between phages and their hosts
69 [15]. For instance, phage specificity, known as precisely targeting the bacterial strain, is
70 regarded as a significant barrier to the successful application of phage therapies [16]. This
71 specificity is directly linked to the key step in recognition between phage receptor-binding
72 proteins (RBP) located on tail fibers, and phage receptors encoded on the susceptible bacterial
73 host cell surface [17]. A common form of developing phage resistance for bacterial hosts is
74 associated with loss or altered structure of the receptors to block the potential phage
75 adsorption in order to avoiding infection [18]. In general, the fitness costs (i.e., motility, nutrient
76 transport or antimicrobial susceptibility) make the mutants unable to compete with phage-
77 susceptible strains in both environmental samples and infection models, even in the presence of
78 phage predation [19, 20]. It is, therefore, crucial to characterize the phage-host interaction
79 regarding the phenotypic and genetic diversification in bacteria and phages prior to any
80 intended phage applications.

81 In this study, we analyzed the molecular epidemiological feature of a collection of 22 clinical
82 *bla*$_{KPC}$ producing *K. pneumoniae* isolates, specifically on the characteristics of ST, plasmid and
83 antibiotic susceptibility. Using these isolates, we isolated and characterize three phages native
84 to hospital sewage. Details of phage host range, genome, morphological characters and phage-
85 host interactions were established to assess the application of phage therapies against the
86 clinical isolates of *K. pneumoniae,* including carbapenem-resistant isolates.

87 **2. Materials and methods**

88 **2.1 Bacterial strains**

89 From December 2019 to January 2020 a total of 22 nonduplicate bacterial isolates of *K.*
90 *pneumoniae* were collected from Zhongshan Hospital, Shanghai, China. *Klebsiella pneumoniae*
91 and *E. coli* were routinely grown in either LB broth with aeration, or, on LB agar plates at 37°C.
92 The beta-lactamase gene (bla_{KPC}) and undecaprenyl-phosphate glucose-1-phosphate transferase
93 gene (*wcaJ*) were detected by PCR and verified using Sanger sequencing (Sango Biotech,
94 Shanghai, China). Oligo sequences are available upon request. Antibiotics were added as
95 necessary to final concentrations, 100 µg/mL apramycin and 100 µg/mL spectinomycin.

96 **2.2 Multi-locus sequence typing (MLST) and antibiotic susceptibility of bacterial isolates**

97 In order to study population genetics and micro-evolution of this epidemic bacteria, MLST was
98 applied to characterize these 22 isolates using sequences of internal fragments of seven house-
99 keeping genes, according to the protocol available on the MLST Pasteur website
100 (https://bigsdb.pasteur.fr/klebsiella/klebsiella.html) [21]. The purified MLST amplicons were
101 sent for Sanger sequencing (Sango Biotech, Shanghai, China), followed by further comparison
102 with those available on the MLST database to determine the sequence type (ST). The VITEK2
103 compact automated system (bioMérieux, Lyon, France) was used to determine antibiotic
104 susceptibility profiles according to the manufacturer's instructions. The susceptibility
105 breakpoints were interpreted with reference to the latest documents from the Clinical and
106 Laboratory Standards Institute (CLSI).

107 **2.3 S1-Pulsed Field Gel Electrophoresis (PFGE)**

108 To characterize the plasmid content in each strain, S1 nuclease digestion analyzed with PFGE
109 was performed as previous described [22]. Briefly, the adjusted bacterial suspension mixed in a
110 1% agarose gel was digested with a proteinase K solution for 2 h at 54°C, then further treated
111 with S1 nuclease. The electrophoresis conditions used in this study were as follows: initial switch

112 time, 3 s; a final switch time, 36 s; gradient, 6 V/cm; angle, 120; temperature, 14°C; and time,
113 18.5 h. After the electrophoresis run was complete, the gel was stained with 1 mg/mL ethidium
114 bromide and visualized with the ChemiDoc XRS system (Bio-Rad Laboratories, CA, USA).

115 **2.4 Isolation and proliferation of phage**

116 Phages were isolated using an enrichment protocol as described previously [23]. Briefly,
117 infiltrated hospital sewage was mixed with the same volume of 2 × LB broth and incubated at
118 37°C for 6 h to stimulate proliferation of total abundances of specific phages targeting the *K.*
119 *pneumoniae* isolates above. Aliquots of enrichment samples were centrifuged (12,000×*g*, 10
120 min) and sterilized with 0.1% chloroform. The presence of *K. pneumoniae*-phages in the hospital
121 sewage samples were detected by double-layer agar assays with different fold dilutions of the
122 cell-free spent supernatant from the enrichment assay. In order to obtain individual phages,
123 single plaques were picked and purified three times with their corresponding hosts. Phage
124 stocks were enriched and titrated using double-layer agar assays as described previously, and
125 stored at 4°C before use [24].

126 **2.5 Phage-host range assay**

127 Phage host range were determined by spot assays. Aliquots of 2 µL phage lysate, approximately
128 10^9 PFU ml^{-1}, was spotted on lawns containing 4 mL top agar mixed with 300 µL mid-log phase
129 bacteria. After incubating at 37°C for 12 h, the spots were assessed by the turbidity of plaques
130 and characterized as strong infection (clear), weak infection (turbid) or no inhibition (no plaque).

131 **2.6 Susceptibility of strain ZS15 to phage infection and isolation of phage-resistant mutants**

132 Overnight (O/N) bacterial cultures were 1,000-fold diluted into LB broth and grown to an
133 exponential phase with an OD600 at 0.3 and infected with its corresponding phage at a MOI of

134 0.01. The suspension was incubated at 37°C with aeration and samples were harvested at 1-h
135 intervals. The phage lysis efficiency was determined by optical density measurements. The
136 experiment was done in triplicate along with parallel control cultures without phages. At
137 timepoint 8- h, phage lysates were streaked on to LB agar plates and individual colonies were
138 subsequentially purified to determine phage susceptibility by spot test assays as described
139 above.

140 **2.7 Phage DNA extraction, genomic analysis, DNA manipulation and complementation assay**

141 For the extraction of phage DNA, 2 mL aliquots of phage lysate with a titer of approximately 10^9
142 PFU mL^{-1} was digested with DNase I and RNase to remove any residual bacterial genomic DNA
143 and RNA according to the manufacturer's protocol [25]. After digesting for 1.5 h at 37°C, EDTA
144 was added to a final concentration of 20 mM to inactivate DNase I and RNase. Total phage DNA
145 was extracted using the Qiagen DNeasy Blood and Tissue kit (Qiagen, CA, USA). Genomic DNA
146 was sent to Sangon Biotech (Shanghai, China) and sequenced using an Illumina HiSeq sequencer.
147 Comparative genomic approaches were used for identifying phage-host interactions in *K.*
148 *pneumoniae* according to previous studies [26, 27].

149 For Δ*wcaJ* mutant construction and complementation assays, the pSGKP-spe-wcaJ, pCasKP and
150 pBAD33-wcaJ plasmids were constructed as described previously and by using the same oligos
151 as in previous studies [27-29]. *Klebsiella pneumoniae* cells were made electrocompetent as
152 follows. O/N cultures were diluted 1:1000 and grown to an OD600 nm between 0.3 and 0.6. A
153 volume of 1.5 mL of culture per transformation was pelleted by centrifugation at 8,000×g for 3
154 min at 4°C. Pellets were washed 3 times in 10% glycerol and finally resuspended in 150 µL 10%
155 glycerol. Plasmids were transferred using a Bio-Rad Micropulser (EC2). Mutants were selected

156 from LB plates containing the corresponding antibiotics, which were further verified by PCR and
157 DNA sequencing to check if they contained the desired mutations.

158 **2.8 Bacteriophage morphology by TEM**

159 Based on the genomic differences, phages were selected for examination by transmission
160 electron microscopy (TEM). Phage stocks were back-diluted in a SM buffer (50 mM Tris-Cl, pH
161 7.5, 99 mM NaCl, 8 mM $MgSO_4$, 0.01% gelatin) to a titer of 10^8 PFU/mL. Diluted phage lysates
162 were then placed on the surface of Formvar carbon-coated grids (Sigma-Aldrich, St. Louis, MO,
163 USA) for 5 min to allow adsorption. Grids were stained with 2% sodium phosphotungstate for 2
164 min prior to being washed in a drop of distilled water and air-dried before being examined using
165 a JEM-2100 microscope operated at 80 kV.

166 **3. Results and Discussion**

167 **3.1 Isolation and characterization of *Klebsiella pneumoniae* strains**

168 Emergence of carbapenem-resistant *K. pneumoniae* (CRKP) has become one major burden of
169 healthcare-associated infection in Chinese hospitals due to the dispersion of bacteria carrying
170 the bla_{KPC} gene [30]. KPC was first found in carbapenem-resistant *K. pneumoniae* strains in 2001
171 in North America, and now KPC-producing *K. pneumoniae* can be frequently isolated from
172 nosocomial samples. It is, therefore, essential to determine and characterize the nosocomial
173 spread of KPC clones and their corresponding phenotype and genotype. Together, a
174 phylogenetically diverse panel of 22 *K. pneumoniae* strains were recovered from various clinical
175 specimens at Zhongshan Hospital, Shanghai, China. According to the *K. pneumoniae* MLST
176 database, all of the 22 clinical isolates belonged to ST11, which is the predominant clone of KPC-
177 producing *K. pneumoniae* in China (Table 1). Despite more than 100 different sequence types

178 (STs) being reported worldwide, the mass dissemination of carbapenemase-producing *K.*
179 *pneumoniae* (KPC-Kp) has been restricted largely to ST258, ST11, ST340 and ST512 [31].

180 In addition, the bla_{KPC} gene was detected in 18 out of 22 (~81%) isolates, indicating the
181 prevalence of β-lactamase nosocomial pathogens (Table 1). The bla_{KPC} gene can be disseminated
182 between species by horizontal (lateral) gene transfer (HGT) via various means, such as plasmids,
183 transposons, prophages and integrative conjugative elements (ICEs), which play an important
184 effect in generating genotypic heterogeneity and phenotypic variation among bacterial
185 populations [32, 33]. For instance, transfer of interspecies KPC can occur through the
186 dissemination of mobile genetic elements between strains of *Staphylococcus aureus* [34].

187 Since pathogenicity and antimicrobial resistance genes are mainly coded by plasmids, in order to
188 identify the subtypes of *K. pneumoniae* ST11, pulsed-field gel electrophoresis with S1 nuclease
189 (S1-PFGE) were utilized to resolve the prevalence of plasmid fingerprints of all the 22 isolates,
190 particularly large ones, which clustered into seven primary groups (Fig. 1). All groups harbored
191 one to three plasmids, except cluster 7 that did not harbor any plasmid between 20 kbp to 500
192 kbp (strain ZS22). Cluster 1, cluster 2, cluster 5 and cluster 6 comprise the majority of bla_{KPC}
193 producing *K. pneumoniae* strains, while cluster 3, cluster4 and cluster 7 do not harbor any bla_{KPC}
194 gene, despite cluster 3 and 4 carrying multiple plasmids of varying sizes (Fig. 1). Thus, it appears
195 that S1-PFGE is a highly discriminative molecular typing method capable of effectively
196 discriminating heterogeneities of ST11 clones.

197 **3.2 Imipenem and meropenem resistance involve production of β-lactamase**

198 Individual antimicrobial data can be found in Table 1. For ticarcillin/clavulanic acid,
199 piperacillin/tazobactam, cefepime, aztreonam, ciprofloxacin and levofloxacin, drug resistance
200 was detected in all strains. In addition, low percentages of resistance to doxycycline,

201 minocycline, tigecycline, colistin and trimethoprim/sulfamethoxazole were also observed for
202 most strains. Of these, 18 (81.8%) out of the 22 isolates become resistant to both imipenem and
203 meropenem with a MIC of ≥16 μg/mL, while the other 4 (18.2%) were both sensitive to
204 imipenem and meropenem. For these four sensitive isolates, three of them were confirmed by
205 PCR and sequencing to have the bla_{KPC} gene. Interestingly, strain ZS14 harboring bla_{KPC} were
206 susceptible to imipenem and meropenem, perhaps indicating the resistance is associated with
207 changes in gene expression at the mRNA levels.

208 **3.3 Isolation and characterization of phages**

209 Three phages were isolated from local hospital sewage using the enrichment protocol to
210 evaluate the potential of phage therapy as an effective alternative against *K. pneumoniae*
211 strains. The host range of the three phages and their lytic efficiency against all of the 22
212 bacterial isolates were assessed using the spot test assay. All phage lysates formed transparent
213 plaques on strain ZS15, which are considered as an indicator of strong lysis.

214 According to the phage lytic profile, the phage isolates were able to infect all of the 22 bacterial
215 isolates, however, each phage displayed a unique profile in terms of host range patterns and
216 lytic efficiency (Fig. 2). Based on their host susceptibilities, phages were divided into two major
217 groups. Specifically, phage φ3 displayed the largest host range, while phage φ1 and φ2 showed
218 a relative narrow host range, infecting only 50% of the tested *K. pneumoniae* strains (Fig. 2). The
219 host range differences between the phages observed in this study is very likely due to the
220 different phage characterization, i.e., efficiency of adsorption and lytic efficiency in its potential
221 hosts. Due to these differences in phage susceptibility profiles and the limited sample numbers,
222 we do not know to what extent these isolated phages represent the true diversity and structure
223 of local hospital sewage phage communities. Further studies of viral metagenomics that are not

224 dependent on cell culture approaches are needed to help us uncover viral populations in
225 hospital sewage.

226 **3.4 Morphology and genome sequence of phages**

227 Based on transmission electron microscopy (TEM) analysis, all the phages belong to the family
228 *Podoviridae* of *Caudovirales* order based on date provided by the International Committee on
229 Taxonomy of Viruses (ICTV), having short, non-contractile tails and icosahedral heads (Fig. 3). In
230 addition, total genomic DNA was extracted from each of the three phages, and their genomes
231 were sequenced by Illumina MiSeq. The assembly sizes of these three phages ranged from 38 kb
232 to 40 kb, having a G+C content ranging between 50% to 53%, with 45 to 49 predicted protein-
233 coding genes (Table 2). All phage genomes (GenBank accession: phage 1, MT813140; phage 2,
234 MT813141; and phage 3, MT813142) were submitted to RAST (Rapid Annotation using
235 Subsystem Technology) and further annotated by the available pipeline. No identifiable virulent
236 genes, antibiotic resistance genes or genes involved in lysogenic cycles were detected.
237 Therefore, it appears that those phages isolated in this study can satisfy the safety assessment
238 based on their complete genome sequences.

239 **3.5 Phage growth characteristics in LB broth**

240 To examine the efficiency of phage infection, *K. pneumoniae* ZS15 was infection in liquid
241 cultures with individual phages (phage φ1, φ2 and φ3) at an MOI of 0.01, respectively, and their
242 inhibition was assessed by bacterial growth following the measurement of the optical density of
243 the bacterial cultures with and without phages. Phage-amended cultures showed similar lytic
244 potential of the 3 phages, with a drastic decline in optical density on the initial control of the
245 host population for 1.5 h followed by regrowth of the resistant population (Fig. 4). A similar
246 inhibitory effect of phage 1 and phage 2 was observed in the *in vitro* inhibition assay, with

247 significant difference of OD values among phage 1, phage 2 and phage 3-amended cultures (Fig.
248 4). Specifically, phage 3 was slightly more effective against the host than the rest of the phages
249 after 5 h. After 8 h, the OD600 nm of the phage-amended cultures of group 1 (ZS15+phage 1
250 and ZS15+phage 2) and group 2 (ZS15+phage 3) stabilized at 1.96 and 0.09, respectively,
251 corresponding to 52% to 96% of the final OD in the control group, respectively (Fig. 4).

252 Despite *K. pneumoniae* ZS15 displaying a strong susceptibility to infection by all three phages,
253 phage 3 was better at suppressing resistance to host strain ZS15 over phage 1 and 2. Bacteria
254 are known to rapidly develop phage-resistance when subjected to predation by lytic phages in
255 laboratory medium [18]. By screening phage resistance mutants, we attempted to better
256 understand the inhibition differences among each of the phage-amended cultures. Phage
257 insensitive mutants were isolated from phage lysate cultures during the incubation for the
258 analysis of changes in their susceptibility upon phage selection. Based on the results of spot test
259 assays, we observed that phage-amended cultures (ZS15+phage 1, ZS15+phage 2, and
260 ZS15+phage 3) were dominated by resistant non-mucoid clones after 8 h of incubation,
261 indicating conversion of mucoid *K. pneumoniae* strain ZS15 to non-mucoid variants by
262 consequence of selective pressure operated by phages. However, in the ZS15+phage 3 cultures,
263 heterogeneity in phage suspibilitiy was observed. Out of 30 phage lysate isolates, two (~6%)
264 were fully sensitive to phage 3 and displayed the hypermucoviscosity (HV) phenotype as the
265 parental strain ZS15. Moreover, a small fraction (~30%) of phage 3 resistant mutants reverted
266 back to the parental phenotype after three rounds of purification. Partially sensitive (i.e.,
267 reduced phage susceptibly when compared to the parental strain) subpopulations (~50%) were
268 isolated as well and did not revert back to the wild type phenotype despite three rounds of
269 purification. Only ~20% were fully resistant to phage 3, suggesting different anti-phage
270 mechanisms were allowing coexistence of phage sensitive mutants and that their lytic phages

271 could exist between bacterial host ZS15 and phage 3. Since phage susceptibility was only
272 measured at 8 h, we do not know the dynamics of phenotype heterogeneity over time or how
273 long such persistence can last before heritage mutations dominate the entire population.

274 **3.6 Identification of genes promoting phage resistance and complementation analysis**

275 To address the underlying mechanism providing bacterial protection against phage predation,
276 12 independently selected spontaneous phage-resistant mutants (four for each phage) and their
277 corresponding wild-type parental strain (ZS15) were subjected to genome extraction, whole
278 genome resequencing and mapped to the ZS15 reference genome (GenBank accession
279 GCA_014050205.1). High-probability mutations, such as high-frequent, non-synonymous
280 mutations within an open reading frame were subject to further screening.

281 Out of 12 phage-resistant mutants, nine harbored mutations in gene *wcaJ*. These nine
282 representative mutants were confirmed by PCR and Sanger sequencing, implying that *wcaJ*
283 mutation is a key contributor to phage resistance. This is consistent with our previous study
284 demonstrating that phage 117 used colanic acid as a phage receptor, mutating the *wcaJ* gene
285 which is the initial enzyme catalyzing the biosynthesis of colanic acid, affecting phage adsorption
286 processes [27, 35]. These results also parallel results for *K. pneumoniae* K7 isolates from Cai et
287 al., in which they found deletion of *wcaJ* could block phage GH-K3 infections [36].

288 Notably, we found that a small fraction (efficiency of plating, EOP<0.01%) of phage 3 still could
289 infect ZS15-3R and ZS15 Δ*wcaJ* cells, respectively, suggesting other mutations may play an
290 important role in providing phage φ3 resistance in addition to *wcaJ* (Fig. 5). These results open
291 the possibilities that phage 3 may use a primary receptor to initiate attachment but require a
292 secondary cell surface receptor to irreversibly bind to the bacterial host for injection. For
293 example, T4 uses its six, long tail fibers to recognize lipopolysaccharide and the outer membrane

294 protein C, present on the bacterial surface. This reversible attachment allows the phage to move
295 along the surface and find a suitable site to inject its DNA [37].

296 Based on our phage-host range spectrum analyses, we noticed 11 strains (50%) among the 22
297 isolates that were fully resistant to phage 1 and phage 2. Next, we determined if these 11
298 resistant isolates harbored a functional *wcaJ* gene or not. As expected, PCR results showed that
299 4 out of 11 resistant isolates did not contained a *wcaJ* gene, displaying full resistance to phage 1
300 and phage2, while being partially susceptible to phage 3 with a decreased EOP, again supporting
301 the previous data and being in line with the phage susceptibility of the Δ*wcaJ* mutant (Fig. 2).
302 Interestingly, we also found seven isolates contained an intact *wcaJ* gene while displaying full
303 resistance to phage 1 and phage 2, which was probably due to the complex nature of colanic
304 acid biosynthesis and mutations in other genes involved for phage adsorption or subsequent
305 steps of phage replication.

306 To test whether there are any other mutations involved in the phages (φ1, φ2, and φ3)
307 resistance, we cloned the wild-type *wcaJ* gene from strain ZS15 into the expression vector
308 pBAD33. The resulting construct was transformed into DH5α competent cells and further
309 electrophorized into *K. pneumoniae* ZS15- 1R, ZS15- 2R and ZS15- 3R to complement the
310 mutation *in trans*. Susceptibilities to the infections of the phages (φ1, φ2, and φ3) were
311 restored, confirming that *wcaJ* mutation was responsible for the phage resistance phenotype
312 (Fig. 5).

313 Taken together, we find that coevolution between the virulent phages and the dominant clone
314 of *K. pneumoniae* ST11 is an indication that perhaps most pervasive phages are extremely well
315 adapted to its host, specially, by using colanic acid as their own receptor and further driving
316 bacterial evolution by selecting phage-resistant mutants that leads to dynamics of an arm race.

317 Understanding the evolutionary implication of phage-colanic acid interactions will be beneficial
318 for predicting how phages interact with their host, as these colanic acid -related phage
319 resistance-mediated phenotypic variabilities may result in exopolysaccharide associated
320 antigenicity and virulence. Such characterization of phage resistance evolution will be used as a
321 guide for selecting proper phage targeting of specific receptors with a significant clinical
322 application. However, the isolated bacteria and phages may only represent a small fraction of
323 the true genomic diversity present in local environments.

324 **3.7 Anti-phage defense-mediated altered sensitivity to antibiotics**

325 Previous studies have shown that evolutionary phage-host interactions affect phage resistance
326 and antibiotic susceptibility both positively and negatively, and are highly genotype-dependent
327 in bacterial populations [38-40]. We started to question whether phage-resistant mutants
328 changed their antibiotic susceptibilities via antagonistic coevolution between hosts and
329 parasites in LB broth. To investigate this further, we performed Vitek 2 assays for antimicrobial
330 susceptibility, testing phage-resistant mutants (ZS15-3R) and their parental phage susceptible
331 strains (ZS15). Interestingly, for tigecycline susceptibility testing of carbapenem-resistant *K.*
332 *pneumoniae* ZS15 strain, we noticed that strain ZS15 evolved resistance to phage 3, while
333 simultaneously becoming more sensitive to tigecycline with the minimum inhibitory
334 concentration shifting from 8 µg/mL to 2 µg/mL. Tigecycline, known as a tetracycline antibiotic,
335 has shown the greatest antimicrobial activity against CRKP. However, genes e.g. *tet*(B), *tet*(A),
336 *tet*(K), *tet*(M) and *tet*(S) coding for multidrug efflux pumps are membrane-related proteins and
337 can efflux tetracyclines from the bacteria intracellularly, thus decreasing the MIC and
338 subsequently allowing protein synthesis without affecting cell viability [41]. Using membrane-
339 related proteins as a surface structure are one of the most common components functioning as
340 a phage receptor. Therefore, it makes sense that phage-resistant defense strategies would

341 confer a fitness cost for bacteria, i.e., becoming more sensitive to certain antibiotics. For
342 instance, in *P. aeruginosa*, phage OMKO1 evolved to become less resistant to antibiotics.
343 Likewise, in *E. coli*, the TolC protein evolved in a variety of diverse cellular functions, including
344 antibiotic efflux and phage TLS receptor [39]. However, unlike previous studies, the anti-phage
345 TLS mediated TolC mutation did not influence its role in antibiotic efflux. Overall, these results
346 reveal that a phage-host arm race can result in different outcomes in terms of antibiotic
347 susceptibilities, highlighting the diversity and complexity of host-interactions within bacterial
348 populations.

349 **4. Conclusion**

350 Successful application of phage therapy requires collaboration between microbiology and
351 preclinical development; however, little is known about their alignment to guide future
352 development. Since the discovery of phages by Frederick W. Twort in Great Britain (1915) and
353 Félix d'Hérelle in France (1917), many phages have been isolated and identified as potential
354 alternatives to antibiotics with different efficacy profiles. Phage specificity is both a benefit and
355 an obstacle for clinical trials, as phage receptor diversity affects phage-host interaction. When
356 the bacterial population is under phage attack, only a small fraction of cells can survive these
357 selective pressures, and those that survive determine the fate of the population. Therefore,
358 elucidating mechanistic details of phage-host interactions and how these would influence
359 bacterial physiological heterogeneity is fundamental to the development of phage therapies. In
360 this study, the three highlighted phages showed promising *in vitro* effects that perhaps these
361 phages can be tamed for our benefits without negatively affecting their natural balance. Further
362 clinical phage therapy trials are still needed to fill our knowledge gap between *in vitro* and *in*
363 *vivo* models.

364 **Acknowledgments**

365 We thank Prof Hongyu Ou, Shanghai Jiao Tong University, Shanghai, China, for kindly providing
366 plasmid pBAD33 and Prof. Quanjiang Ji, Shanghai Tech University, Shanghai, China, for proving
367 plasmid pCasKP-apr and pSGKP-spe. We are grateful to Brett C. Gonzalez for proofreading the
368 manuscript.

369 **Funding**

370 This study was supported by Shanghai Public Health Clinical Center, Fudan University (SJTNY and
371 KY-GW-2020-08), National Natural Science Foundation of China (82072325) and Shanghai
372 Municipal Health Bureau, Shanghai, China (20204Y0336).

373 **Conflict of interest**

374 None declared.

375 **References**

376 [1] Ventola CL. The antibiotic resistance crisis: part 1: causes and threats. P T. 2015;40:277-83.
377 [2] Pendleton JN, Gorman SP, Gilmore BF. Clinical relevance of the ESKAPE pathogens. Expert
378 Rev Anti Infect Ther. 2013;11:297-308.
379 [3] Pitout JD, Sanders CC, Sanders Jr WEJTAjom. Antimicrobial resistance with focus on β-lactam
380 resistance in gram-negative bacilli. 1997;103:51-9.
381 [4] Suttle CA. Viruses in the sea. Nature. 2005;437:356-61.
382 [5] Sulakvelidze A, Alavidze Z, Morris JG, Jr. Bacteriophage therapy. Antimicrob Agents
383 Chemother. 2001;45:649-59.
384 [6] Hung CH, Kuo CF, Wang CH, Wu CM, Tsao N. Experimental phage therapy in treating
385 Klebsiella pneumoniae-mediated liver abscesses and bacteremia in mice. Antimicrob Agents
386 Chemother. 2011;55:1358-65.
387 [7] Schooley RT, Biswas B, Gill JJ, Hernandez-Morales A, Lancaster J, Lessor L, et al. Development
388 and use of personalized bacteriophage-based therapeutic cocktails to treat a patient with a
389 disseminated resistant Acinetobacter baumannii infection. 2017;61.
390 [8] Letkiewicz S, Międzybrodzki R, Fortuna W, Weber-Dąbrowska B, Górski AJFm. Eradication of
391 Enterococcus faecalis by phage therapy in chronic bacterial prostatitis—case report.
392 2009;54:457.
393 [9] Capparelli R, Parlato M, Borriello G, Salvatore P, Iannelli D. Experimental phage therapy
394 against Staphylococcus aureus in mice. Antimicrob Agents Chemother. 2007;51:2765-73.

395 [10] McVay CS, Velasquez M, Fralick JA. Phage therapy of Pseudomonas aeruginosa infection in
396 a mouse burn wound model. Antimicrob Agents Chemother. 2007;51:1934-8.
397 [11] Chibani-Chennoufi S, Sidoti J, Bruttin A, Kutter E, Sarker S, Brussow H. In vitro and in vivo
398 bacteriolytic activities of Escherichia coli phages: implications for phage therapy. Antimicrob
399 Agents Chemother. 2004;48:2558-69.
400 [12] Cano EJ, Caflisch KM, Bollyky PL, Van Belleghem JD, Patel R, Fackler J, et al. Phage Therapy
401 for Limb-threatening Prosthetic Knee Klebsiella pneumoniae Infection: Case Report and In Vitro
402 Characterization of Anti-biofilm Activity. 2020.
403 [13] Abd El-Aziz AM, Elgaml A, Ali YM. Bacteriophage Therapy Increases Complement-Mediated
404 Lysis of Bacteria and Enhances Bacterial Clearance After Acute Lung Infection With Multidrug-
405 Resistant Pseudomonas aeruginosa. J Infect Dis. 2019;219:1439-47.
406 [14] Dedrick RM, Guerrero-Bustamante CA, Garlena RA, Russell DA, Ford K, Harris K, et al.
407 Engineered bacteriophages for treatment of a patient with a disseminated drug-resistant
408 Mycobacterium abscessus. Nature medicine. 2019;25:730.
409 [15] Chibani-Chennoufi S, Bruttin A, Dillmann ML, Brussow H. Phage-host interaction: an
410 ecological perspective. J Bacteriol. 2004;186:3677-86.
411 [16] Koskella B, Meaden S. Understanding bacteriophage specificity in natural microbial
412 communities. Viruses. 2013;5:806-23.
413 [17] Bertozzi Silva J, Storms Z, Sauvageau D. Host receptors for bacteriophage adsorption. FEMS
414 Microbiol Lett. 2016;363.
415 [18] Labrie SJ, Samson JE, Moineau S. Bacteriophage resistance mechanisms. Nat Rev Microbiol.
416 2010;8:317-27.
417 [19] Seed KD, Faruque SM, Mekalanos JJ, Calderwood SB, Qadri F, Camilli A. Phase variable O
418 antigen biosynthetic genes control expression of the major protective antigen and
419 bacteriophage receptor in Vibrio cholerae O1. PLoS Pathog. 2012;8:e1002917.
420 [20] Sumrall ET, Shen Y, Keller AP, Rismondo J, Pavlou M, Eugster MR, et al. Phage resistance at
421 the cost of virulence: Listeria monocytogenes serovar 4b requires galactosylated teichoic acids
422 for InlB-mediated invasion. 2019;15:e1008032.
423 [21] Diancourt L, Passet V, Verhoef J, Grimont PA, Brisse S. Multilocus sequence typing of
424 Klebsiella pneumoniae nosocomial isolates. J Clin Microbiol. 2005;43:4178-82.
425 [22] Tan D, Zhang Y, Cheng M, Le S, Gu J, Bao J, et al. Characterization of Klebsiella pneumoniae
426 ST11 isolates and their interactions with lytic phages. 2019;11:1080.
427 [23] Tan D, Gram L, Middelboe MJA, microbiology e. Vibriophages and their interactions with
428 the fish pathogen Vibrio anguillarum. 2014;80:3128-40.
429 [24] Kropinski AM, Mazzocco A, Waddell TE, Lingohr E, Johnson RP. Enumeration of
430 Bacteriophages by Double Agar Overlay Plaque Assay. In: Clokie MRJ, Kropinski AM, editors.
431 Bacteriophages: Methods and Protocols, Volume 1: Isolation, Characterization, and Interactions.
432 Totowa, NJ: Humana Press; 2009. p. 69-76.
433 [25] Jakočiūnė D, Moodley A. A Rapid Bacteriophage DNA Extraction Method. 2018;1:27.
434 [26] Le S, Yao X, Lu S, Tan Y, Rao X, Li M, et al. Chromosomal DNA deletion confers phage
435 resistance to Pseudomonas aeruginosa. Sci Rep. 2014;4:4738.
436 [27] Tan D, Zhang Y, Qin J, Le S, Gu J, Chen LK, et al. A Frameshift Mutation in wcaJ Associated
437 with Phage Resistance in Klebsiella pneumoniae. Microorganisms. 2020;8:378.
438 [28] Wang Y, Wang S, Chen W, Song L, Zhang Y, Shen Z, et al. CRISPR-Cas9 and CRISPR-Assisted
439 Cytidine Deaminase Enable Precise and Efficient Genome Editing in Klebsiella pneumoniae. Appl
440 Environ Microbiol. 2018;84.

441 [29] Qian H, Yu H, Li P, Zhu E, Yao Q, Tai C, et al. Toxin–antitoxin operon kacAT of Klebsiella
442 pneumoniae is regulated by conditional cooperativity via a W-shaped KacA–KacT complex.
443 2019;47:7690-702.
444 [30] Bush K, Bradford PAJCSHpim. β-Lactams and β-lactamase inhibitors: an overview.
445 2016;6:a025247.
446 [31] Pitout JD, Nordmann P, Poirel L. Carbapenemase-Producing Klebsiella pneumoniae, a Key
447 Pathogen Set for Global Nosocomial Dominance. Antimicrob Agents Chemother. 2015;59:5873-
448 84.
449 [32] Hardiman CA, Weingarten RA, Conlan S, Khil P, Dekker JP, Mathers AJ, et al. Horizontal
450 Transfer of Carbapenemase-Encoding Plasmids and Comparison with Hospital Epidemiology
451 Data. Antimicrob Agents Chemother. 2016;60:4910-9.
452 [33] Botelho J, Schulenburg H. The Role of Integrative and Conjugative Elements in Antibiotic
453 Resistance Evolution. Trends Microbiol. 2020.
454 [34] Goren MG, Carmeli Y, Schwaber MJ, Chmelnitsky I, Schechner V, Navon-Venezia S. Transfer
455 of carbapenem-resistant plasmid from Klebsiella pneumoniae ST258 to Escherichia coli in
456 patient. Emerg Infect Dis. 2010;16:1014-7.
457 [35] Patel KB, Toh E, Fernandez XB, Hanuszkiewicz A, Hardy GG, Brun YV, et al. Functional
458 characterization of UDP-glucose:undecaprenyl-phosphate glucose-1-phosphate transferases of
459 Escherichia coli and Caulobacter crescentus. J Bacteriol. 2012;194:2646-57.
460 [36] Cai R, Wang G, Le S, Wu M, Cheng M, Guo Z, et al. Three Capsular Polysaccharide Synthesis-
461 Related Glucosyltransferases, GT-1, GT-2 and WcaJ, Are Associated With Virulence and Phage
462 Sensitivity of Klebsiella pneumoniae. Front Microbiol. 2019;10:1189.
463 [37] Islam MZ, Fokine A, Mahalingam M, Zhang Z, Garcia-Doval C, van Raaij MJ, et al. Molecular
464 anatomy of the receptor binding module of a bacteriophage long tail fiber. PLOS Pathogens.
465 2019;15:e1008193.
466 [38] Comeau AM, Tétart F, Trojet SN, Prere M-F, Krisch HJPo. Phage-antibiotic synergy (PAS): β-
467 lactam and quinolone antibiotics stimulate virulent phage growth. 2007;2:e799.
468 [39] Chan BK, Sistrom M, Wertz JE, Kortright KE, Narayan D, Turner PE. Phage selection restores
469 antibiotic sensitivity in MDR Pseudomonas aeruginosa. Sci Rep. 2016;6:26717.
470 [40] Burmeister AR, Fortier A, Roush C, Lessing AJ, Bender RG, Barahman R, et al. Pleiotropy
471 complicates a trade-off between phage resistance and antibiotic resistance. 2020;117:11207-16.
472 [41] Linkevicius M, Sandegren L, Andersson DI. Potential of Tetracycline Resistance Proteins To
473 Evolve Tigecycline Resistance. Antimicrob Agents Chemother. 2016;60:789-96.

474

475

476

477

478

479

480 Table 1. MLST types and antibiotic susceptibility profiles of the 22 *Klebsiella pneumoniae* isolates
481 and their corresponding phage-resistant mutants. Antibiotic abbreviations: ticarcillin-clavulanic
482 acid (TIM), piperacillin-tazobactam (TZP), ceftazidime (CAZ), cefoperazone/sulbactam (CPZ/SBT),
483 cefepime (FEP), aztreonam (ATM), imipenem (IPM), meropenem (MEM), amikacin (AMK),
484 tobramycin (TOB), ciprofloxacin (CIP), levofloxacin (LVX), doxycycline (DOX), minocycline (MIN),
485 tigecycline (TGC), colistin (CST), trimethoprim-sulfamethoxazole (SXT).

486 Table 2. Morphological and genomic characterization of phages isolated from the local hospital
487 sewage.

488 Figure 1. Dendrogram generated by BioNumerics software (Version7.1, Applied Maths, St-
489 Martens-Latem, Belgium) showing cluster results of molecular epidemiology S1-PFGE analysis of
490 22 *Klebsiella pneumoniae* isolates. Band-based similarity coefficients were calculated using Dice
491 coefficient and unweighted pair group average method algorithm (UPGMA).

492 Figure 2. Phage-host range assay of the three phages (columns) against the 22 *Klebsiella*
493 *pneumoniae* isolates (rows). *Klebsiella pneumoniae* phages displayed broad and narrow host
494 ranges. Black, grey and white indicate infection, weak infection and no plaque formation,
495 respectively. The presence or absence of *wcaJ* gene of the 22 Klebsiella pneumoniae isolates.

496 Figure 3. Plaque images of phages and their corresponding TEM micrographs. Phages were
497 stained with 2% sodium phosphotungstate and were found to have short small podophage
498 morphology. Scale bar, 200 nm.

499 Figure 4. Inhibition assay of phage 1, phage 2 and phage 3 in the treatment at an MOI of 0.1 and
500 control without phage in cultures of *Klebsiella pneumoniae* ZS15. Optical density (OD600) was
501 measured at 1-h intervals over an 8-h incubation period. Error bars represent the standard
502 deviations from all experiments, carried out in triplicate.

503 Figure 5. Spot test assay of phage 1, phage 2 and phage 3 on the parental *Klebsiella pneuoniae*

504 ZS15 (A) and its derivative strains (B: Δ*wcaJ*, C: ZS15-1R, D: ZS15-1R pBAD33-wcaJ, E: ZS15-2R, F:

505 ZS15-2R pBAD33-wcaJ, G: ZS15-3R and H: ZS15-3R pBAD33-wcaJ)

506

			Minimum inhibitory concentration (μg/mL)																
Strain	MLST	bla_{KPC}	TIM	TZP	CAZ	CPZ	FEP	ATM	IMP	MEM	AMK	TOB	CIP	LVX	DOX	MIN	TGC	CST	SXT
ZS1	ST11	Yes	≥128	≥128	≥64	≥64	≥32	≥64	≥16	≥16	≥64	≥16	≥4	≥8	2	4	≤0.5	≤0.5	≤20
ZS2	ST11	Yes	≥128	≥128	≥64	32	≥32	≥64	≥16	≥16	4	8	≥4	≥8	2	8	1	≥16	≤20
ZS3	ST11	No	≥128	≥128	≥64	≥64	≥32	≥64	1	1	≥64	≥16	≥4	≥8	4	≥16	2	≤0.5	≤20
ZS4	ST11	Yes	≥128	≥128	32	≥64	≥32	≥64	0.5	≤0.25	≥64	≥16	≥4	≥8	2	8	1	≤0.5	≤20
ZS5	ST11	Yes	≥128	≥128	≥64	≥64	≥32	≥64	≥16	≥16	4	≤1	≥4	≥8	8	≥16	4	≤0.5	≤20
ZS6	ST11	Yes	≥128	≥128	≥64	≥64	≥32	≥64	≥16	≥16	≥64	≥16	≥4	≥8	1	2	≤0.5	≤0.5	≤20
ZS7	ST11	Yes	≥128	≥128	≥64	≥64	≥32	≥64	≥16	≥16	4	≤1	≥4	≥8	≥16	≥16	≥8	≤0.5	≤20
ZS8	ST11	Yes	≥128	≥128	≥64	≥64	≥32	≥64	≥16	≥16	≥64	≥16	≥4	≥8	4	8	2	≤0.5	≤20
ZS9	ST11	Yes	≥128	≥128	≥64	≥64	≥32	≥64	≥16	≥16	≥64	≥16	≥4	≥8	4	8	2	≤0.5	≤20
ZS10	ST11	Yes	≥128	≥128	≥64	≥64	≥32	≥64	≥16	≥16	≥64	≥16	≥4	≥8	≥16	≥16	4	4	≥320
ZS11	ST11	Yes	≥128	≥128	≥64	≥64	≥32	≥64	≥16	≥16	≥64	≥16	≥4	≥8	2	8	2	≤0.5	≤20
ZS12	ST11	Yes	≥128	≥128	≥64	≥64	≥32	≥64	≥16	≥16	≥64	≥16	≥4	≥8	2	8	1	≤0.5	≤20
ZS13	ST11	Yes	≥128	≥128	≥64	≥64	≥32	≥64	≥16	≥16	≥64	≥16	≥4	≥8	2	8	≤0.5	≤0.5	≤20
ZS14	ST11	No	≥128	≥128	32	≥64	≥32	≥64	1	0.5	≥64	≥16	≥4	≥8	2	8	≤0.5	≤0.5	≤20
ZS15	ST11	Yes	≥128	≥128	≥64	≥64	≥32	≥64	≥16	≥16	≥64	≥16	≥4	≥8	2	8	≥8	≤0.5	≤20
ZS16	ST11	Yes	≥128	≥128	≥64	≥64	≥32	≥64	≥16	≥16	≥64	≥16	≥4	≥8	4	≥16	2	≥16	≤20
ZS17	ST11	Yes	≥128	≥128	≥64	≥64	≥32	≥64	≥16	≥16	≥64	≥16	≥4	≥8	4	8	1	≤0.5	≤20
ZS18	ST11	Yes	≥128	≥128	≥64	32	≥32	≥64	≥16	8	8	≤1	≥4	≥8	≤0.5	2	≤0.5	≤0.5	≤20
ZS19	ST11	No	≥128	≥128	8	≥64	≥32	≥64	≤0.25	≤0.25	≥64	≥16	≥4	≥8	2	4	≤0.5	≤0.5	≤20
ZS20	ST11	Yes	≥128	≥128	≥64	≥64	≥32	≥64	≥16	≥16	≥64	≥16	≥4	≥8	1	4	≤0.5	≤0.5	≤20
ZS21	ST11	Yes	≥128	≥128	≥64	≥64	≥32	≥64	≥16	≥16	≥64	≥16	≥4	≥8	1	4	≤0.5	≤0.5	≤20
ZS22	ST11	Yes	≥128	≥128	≥64	≥64	≥32	≥64	≥16	≥16	≥64	≥16	≥4	≥8	1	2	≤0.5	≤0.5	≤20

Phage	Family	Host	Head diam (nm)	Head length (nm)	Tail diam (nm)	Tail length (nm)	Genome size (bp)	GC%	Genome type	Predicted genes	Phage receptor	Source
Φ1	Podoviridae	ZS15	63	58	13	14	40,428	53	dsDNA	45	Colanic acid	Sewage
Φ2	Podoviridae	ZS15	58	63	13	9	40,222	52.8	dsDNA	49	Colanic acid	Sewage
Φ3	Podoviridae	ZS15	63	63	13	11	38,741	50.7	dsDNA	46	Colanic acid	Sewage

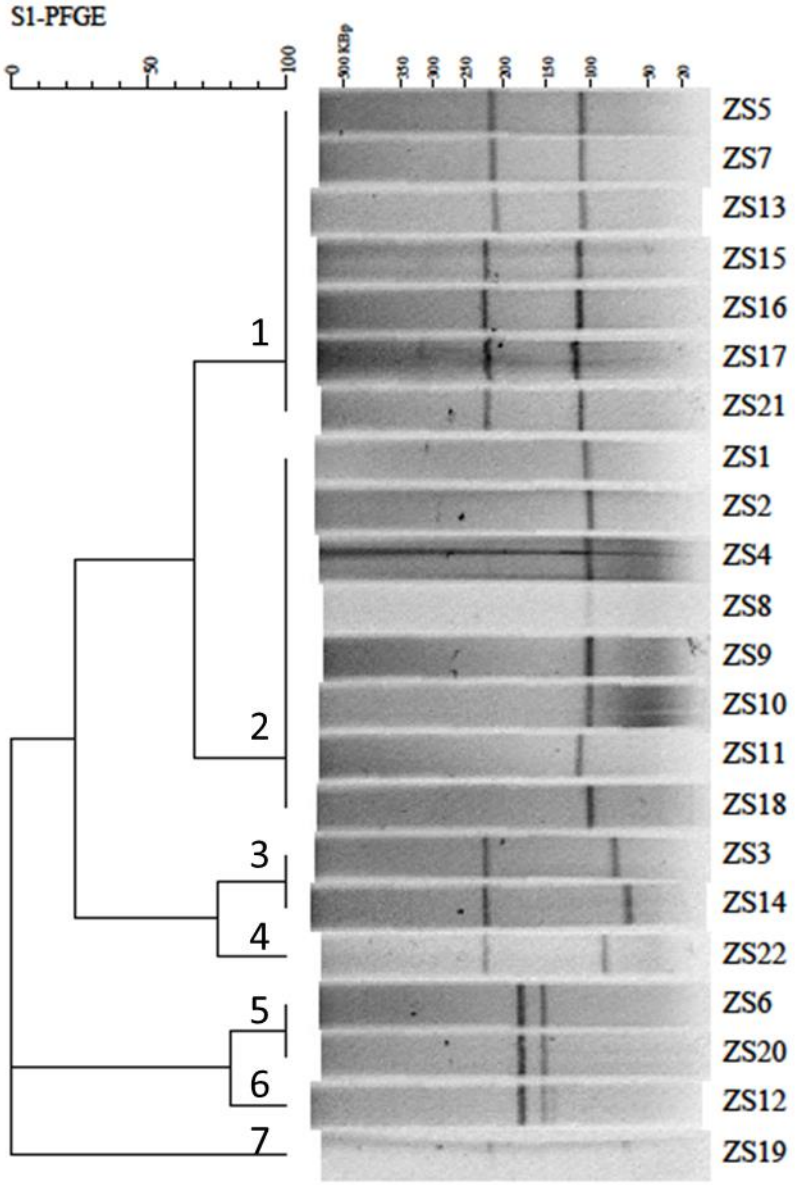
S1-PFGE
0
50
100
500 KBp
350
300
250
200
150
100
50
20
1
2
3
4
5
6
7
ZS5
ZS7
ZS13
ZS15
ZS16
ZS17
ZS21
ZS1
ZS2
ZS4
ZS8
ZS9
ZS10
ZS11
ZS18
ZS3
ZS14
ZS22
ZS6
ZS20
ZS12
ZS19

Strain	Phage			*wcaJ* gene
	Φ1	Φ2	Φ3	
ZS1				Yes
ZS2				Yes
ZS3				Yes
ZS4				Yes
ZS5				Yes
ZS6				No
ZS7				Yes
ZS8				Yes
ZS9				Yes
ZS10				Yes
ZS11				Yes
ZS12				No
ZS13				Yes
ZS14				Yes
ZS15				Yes
ZS16				Yes
ZS17				Yes
ZS18				Yes
ZS19				Yes
ZS20				No
ZS21				No
ZS22				Yes

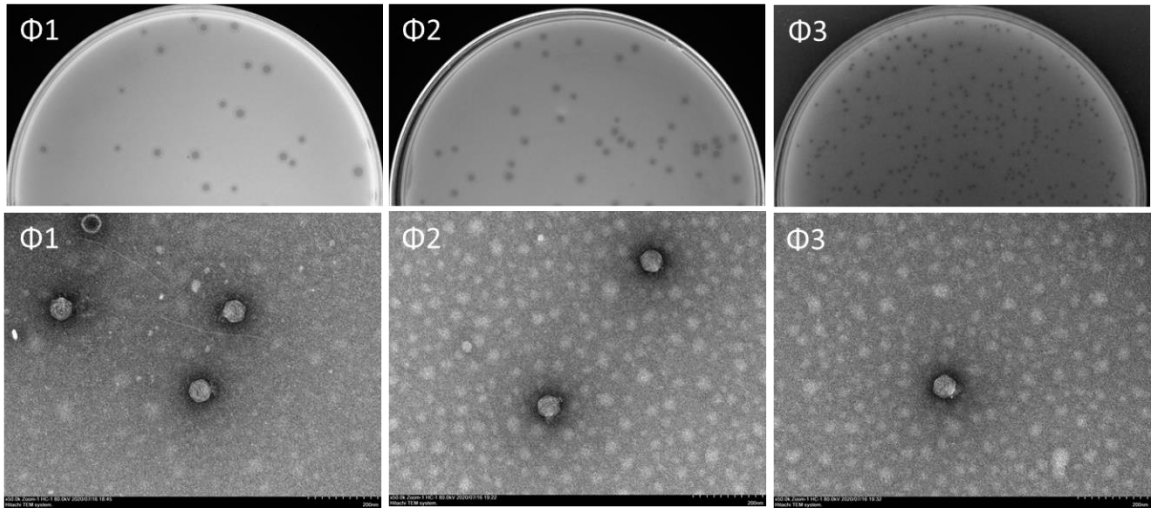
Φ1
Φ2
Φ3
Φ1
Φ2
Φ3

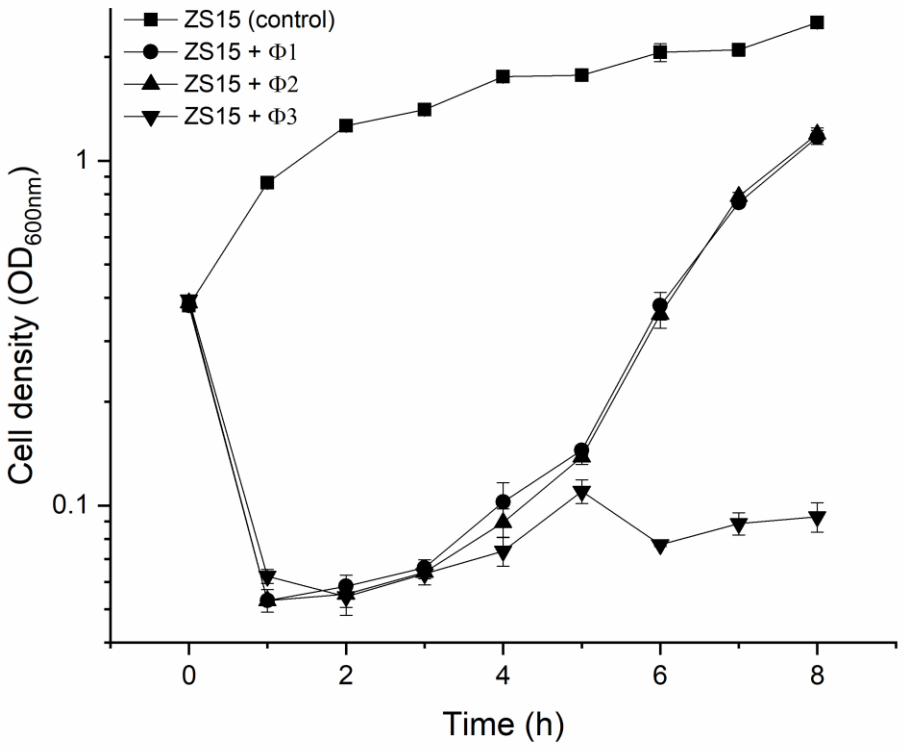
ZS15 (control)
ZS15 + Φ1
ZS15 + Φ2
ZS15 + Φ3
Cell density (OD600nm)
1
0.1
0
2
4
6
8
Time (h)

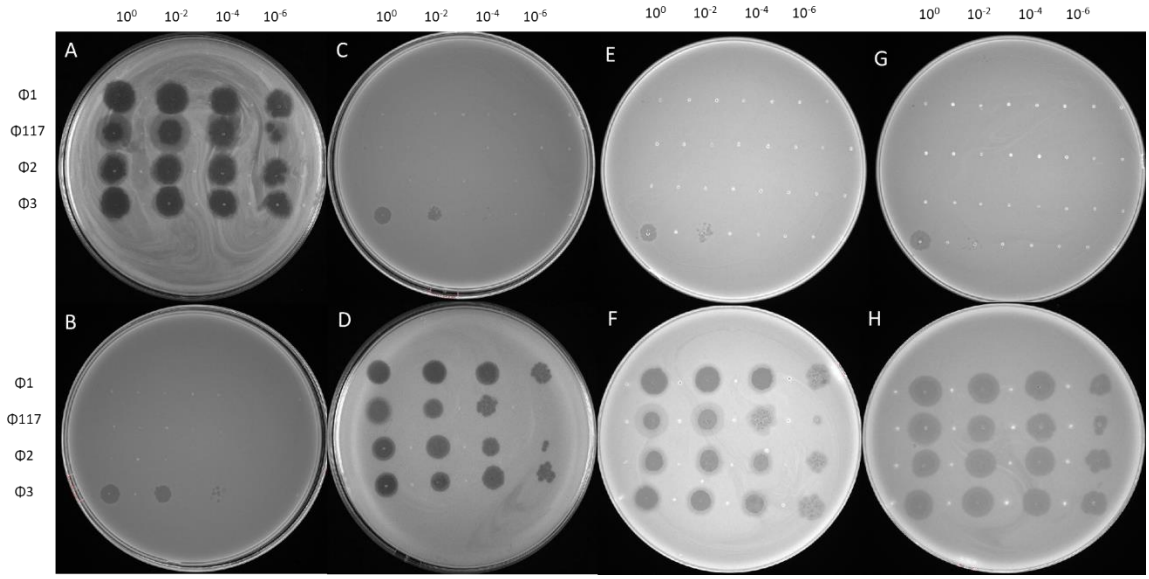
10^0 10^{-2} 10^{-4} 10^{-6}
10^0 10^{-2} 10^{-4} 10^{-6}
10^0 10^{-2} 10^{-4} 10^{-6}
10^0 10^{-2} 10^{-4} 10^{-6}
A
C
E
G
B
D
F
H
Φ1
Φ117
Φ2
Φ3
Φ1
Φ117
Φ2
Φ3